



**HAL**  
open science

## Ice-crystal traces imply ephemeral freezing in early Permian equatorial Pangea

Lily Pfeifer, Brooke Birkett, Jean van den Driessche, Stéphane Pochat,  
Gerilyn Soreghan

► **To cite this version:**

Lily Pfeifer, Brooke Birkett, Jean van den Driessche, Stéphane Pochat, Gerilyn Soreghan. Ice-crystal traces imply ephemeral freezing in early Permian equatorial Pangea. *Geology*, 2021, 49 (11), pp.1397-1401. 10.1130/G49011.1 . hal-03414901

**HAL Id: hal-03414901**

**<https://hal.science/hal-03414901>**

Submitted on 9 Dec 2021

**HAL** is a multi-disciplinary open access archive for the deposit and dissemination of scientific research documents, whether they are published or not. The documents may come from teaching and research institutions in France or abroad, or from public or private research centers.

L'archive ouverte pluridisciplinaire **HAL**, est destinée au dépôt et à la diffusion de documents scientifiques de niveau recherche, publiés ou non, émanant des établissements d'enseignement et de recherche français ou étrangers, des laboratoires publics ou privés.

# Ice-crystal traces imply ephemeral freezing in early Permian equatorial Pangea

Lily S. Pfeifer<sup>1</sup>, Brooke A. Birkett<sup>2</sup>, Jean Van Den Driessche<sup>3</sup>, Stéphane Pochat<sup>4</sup> and Gerilyn S. Soreghan<sup>1</sup>

<sup>1</sup>School of Geosciences, University of Oklahoma, 100 East Boyd Street, Norman, Oklahoma 73019, USA

<sup>2</sup>Geosciences and Geological and Petroleum Engineering Department, Missouri University of Science and Technology, 1400 North Bishop, Rolla, Missouri 65409, USA

<sup>3</sup>Géosciences Rennes—UMR 6118, Université de Rennes, CNRS, F-35000 Rennes, France

<sup>4</sup>Laboratoire de Planétologie et de Géodynamique—UMR 6112, Université de Nantes, CNRS, 2 rue de la Houssinière, F-44000 Nantes, France

## ABSTRACT

**Delicate impressions in lacustrine strata of the lower Permian (lower Cisuralian) Usclas Formation record ephemeral freezing in equatorial Pangea. These sediments accumulated in the paleoequatorial and intramontane Lodève Basin (southern Massif Central, France) during peak icehouse conditions of the Late Paleozoic Ice Age. Experimental replication of these features supports the interpretation that they are ice-crystal molds. Evidence for films of ice in marginal-lacustrine sediment at such low latitudes and inferred low to moderate altitudes (1–2 km) calls for a reevaluation of climate conditions in eastern equatorial Pangea. Ephemeral freezing implies either cold tropical temperatures (~5 °C cooler than the Last Glacial Maximum) and/or lapse rates that exceeded those of the Last Glacial Maximum. Extreme continentality of the Lodève Basin would have amplified seasonality, albeit the climatic forcing(s) necessary to have promoted cold temperatures in equatorial Pangea remain enigmatic.**

## INTRODUCTION

The Graissessac-Lodève Basin is a small continental rift basin in France's Massif Central (Fig. 1). Delicate crystal molds in multiple bedding-plane exposures of the lower Permian Usclas Formation have been interpreted to record traces of either gypsum crystals, implying evaporative conditions (Odin, 1986), or ice crystals, implying ephemeral freezing (Becq-Giraudon et al., 1996) during the Late Paleozoic Ice Age (LPIA). We documented and characterized the primary morphologies of these features and conducted laboratory analyses to empirically reproduce sediment impressions left by freezing of water-saturated mud. The paleoenvironmental conditions of formation (ephemeral freezing) implied by these results demand a reevaluation of climate models in low-latitude, early Permian Pangea.

## BACKGROUND

Pangean assembly resulted in uplift of the Central Pangean Mountains, which spanned the

equator from North America (the Appalachian-Ouachita-Marathon belt) through Western Europe (the Variscan belt). Syn-orogenic extension in the late stages of the Variscan orogeny (ca. 300 Ma) produced several rift basins (Burg et al., 1994) that remained within the equatorial belt throughout the Permo-Carboniferous (Fig. 1; Domeier and Torsvik, 2014; Evans et al., 2014; Kent and Muttoni, 2020). Among them, the Lodève Basin (southern Massif Central) preserves a late Carboniferous–Permian record of regional paleoequatorial climate from apex to collapse of the LPIA.

The frequency of ice-contact deposits across southern Gondwana implies that Asselian–Sakmarian (early Permian; ca. 298–295 Ma) time records the most intense phase of the LPIA (e.g., Soreghan et al., 2019). Semiarid climates and periglacial-proglacial conditions at paleoequatorial latitudes have also been hypothesized in both western (Ancestral Rocky Mountains; Soreghan et al., 2008, 2014) and eastern (Variscan paleomountains; Julien, 1895; Becq-Gi-

raudon et al., 1996; Pfeifer et al., 2020) Pangea. However, these claims remain controversial because they imply colder conditions than models can replicate (e.g., Heavens et al., 2015).

The lower Permian (lower Cisuralian) Usclas Formation (Lodève Basin) consists primarily of organic-rich mudstone and tan siltstone of lacustrine origin (variable water depth; Pochat and Van Den Driessche, 2011). Delicate, stellate features occur on multiple bedding-plane exposures here and in coeval strata of the nearby Gabian-Neffies Basin (Montenat and Dolle, 1986) and Germany (Martinstejn-Nahe; Reineck, 1955). Features with similar attributes—although rare in the geological record (Table 1, and references therein)—have been interpreted as ice-crystal traces, with low-latitude examples dating exclusively from the upper Carboniferous–lower Permian.

## METHODS

We measured three detailed sections of the Usclas Formation (totaling 5.4 m; Fig. 1) containing abundant delicate impressions, at centimeter-scale resolution. The impressions were classified into three morphologies. Thin sections were made of representative samples and compositional analyses (energy dispersive spectroscopy) were acquired with an electron probe microanalyzer. We conducted experiments to freeze mud (saturated with distilled water or dilute NaCl solutions) in order to simulate ice-crystal growth and test the hypothesis that the features represent ice traces (experimental set up and variables are provided in Appendix S1 in the Supplemental Material<sup>1</sup>).

<sup>1</sup>Supplemental Material. Appendices S1–S4. Please visit <https://doi.org/10.1130/GEOL.S.14925237> to access the supplemental material, and contact editing@geosociety.org with any questions.

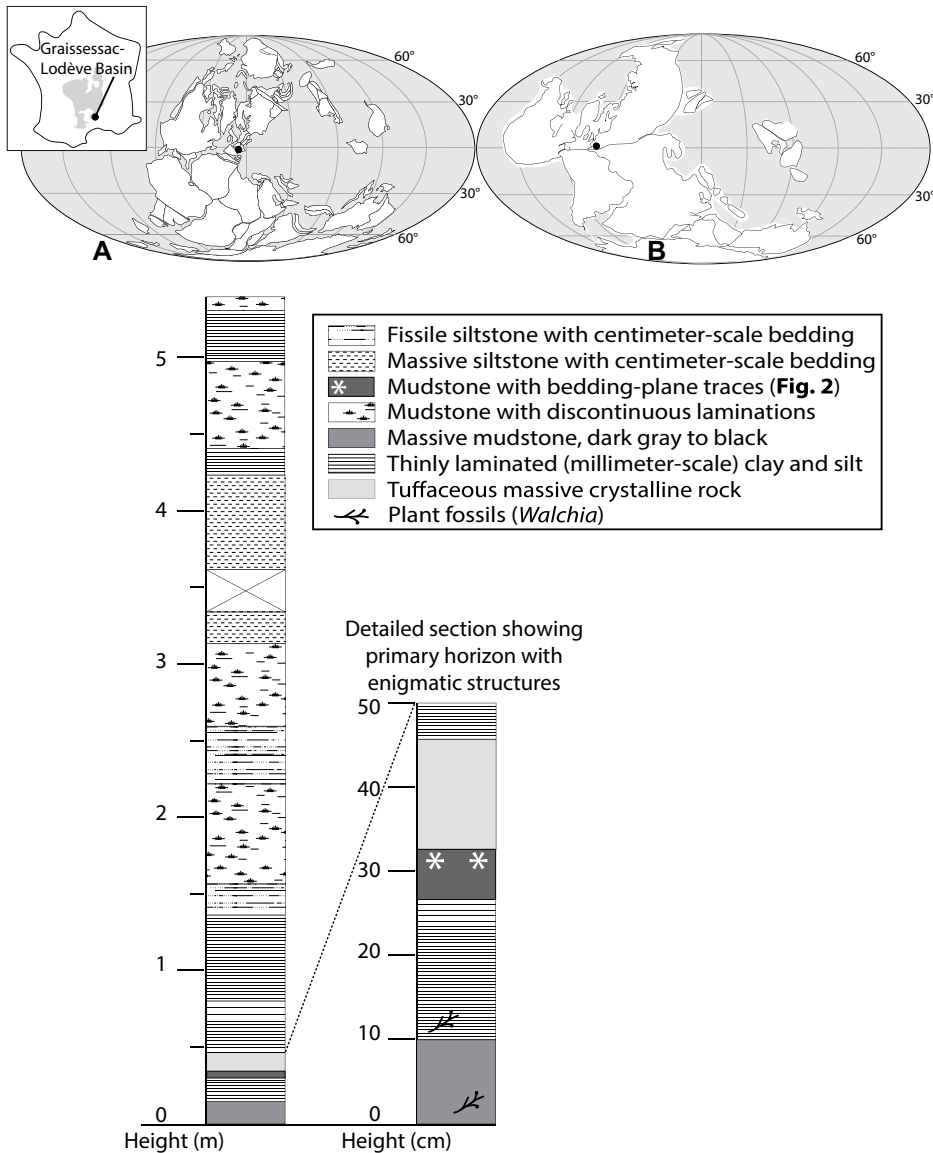


**Figure 1.** (Top) Early Permian (ca. 290 Ma) paleogeographic reconstructions of Domeier and Torsvik (2014) (Pangea, A) and Kent and Muttoni (2020) (Pangea, B). Black dots show equatorial location of the Graissessac-Lodève Basin (southern margin of the French Massif Central; gray shading on inset map) at  $\sim 0^{\circ}$ – $2^{\circ}$ S (A) to  $0^{\circ}$ – $2^{\circ}$ N (B), consistent with published paleomagnetic data from the Lodève Basin (Evans et al., 2014). Proximity to the Paleotethys ocean varies substantially, though both suggest a relatively continental position (e.g., Molli et al., 2020). (Bottom) Stratigraphic section (concatenation of three exposures) of the Usclas Formation, Lodève Basin. Detailed log on right shows bottom 0.5 m at centimeter-scale resolution where most of the enigmatic structures are found (white asterisks).

TABLE 1. SUMMARY OF EXISTING INTERPRETATIONS OF ICE CRYSTAL TRACE MARKINGS (MODERN–ANCIENT)

Time	Location	Paleo-latitude	Paleo-altitude (m)	Substrate	Bed	Citation	Figure S2 panel
Modern	Germany	49.8	SL	mud		Hänzschel, 1935	
Modern	Illinois, USA	41.5	150	loess		Udden, 1918	A
Modern	Northeast USA	42.3	SL	clay		Shaler et al., 1806	
Modern	Northwest Idaho, USA	46.7	500	loess		Mark, 1932	
Modern	Tidal Bay, California, USA	47.3	SL	sand-mud		Dionne, 1985	
Pleistocene	Utah, USA	40.2	1500	fine sands	surface	Mark, 1932	DE
Upper Cretaceous	South Dakota, USA	46.7	SL	silt-clay	surface	Udden, 1918	
Upper Cretaceous	Texas, USA	33.8	SL	lime-clay	surface	Udden, 1918	HI
Middle Permian	New Mexico, USA	9.2	SL	limestone	surface	Lang, 1937	G
Lower Permian	Germany	3.9	$\sim 300$	silt-clay	surface	Reineck, 1955	
Lowe Carboniferous	De L'air, Niger	$-50$	$<300$	mud-silt	surface	Lang et al., 1991	L
Upper Devonian	New York, USA	$-33$	SL	sand-mud	base	Clarke, 1917	
Upper Ordovician	Libya	$-62$	$<300$	mud	surface	Girard et al., 2015	K
Upper Ordovician	Morocco	$-80$	$<300$	sandy mud	surface	Nutz et al., 2013	J

See Appendix S3 (see text footnote 1) for photos and references. Paleolatitudes are converted from modern latitudes using the paleogeography of Torsvik et al. (2012; and the calculator at <http://paleolatitude.org>, and paleoaltitude estimations are approximate. SL—paleoaltitudes around sea level.

## RESULTS

### Morphological Documentation of Delicate Traces

The Usclas Formation (Fig. 1) comprises massive to locally laminated, thinly bedded mudstone to tuffaceous mudstone (mode 25–30  $\mu\text{m}$ ; see Appendix S2). The bedding-plane traces (occurring as both molds and casts) exhibit three morphologies (Fig. 2) designated as “SR” (stubby rods), “FN” (fanned needles), and “DC” (delicate, complex), albeit these represent a continuum. Morphologies FN and DC (most common) co-occur and present as molds. Morphology SR presents as casts. All impressions contain secondary minerals (Fig. 2): Potassium feldspar replaces dolomite in SR, and potassium feldspar lines molds of FN and DC. Morphology SR forms composite, rod-like, stubby needles (6–10 mm), wherein bundles commonly intersect at  $60^{\circ}$ ,  $90^{\circ}$ , or  $180^{\circ}$ . Morphology FN consists of needles (2–5 mm) occurring most commonly as fans radiating at  $60^{\circ}$ – $120^{\circ}$ ; less common are feather-like features (as long as 20–25 mm) that fan in preferred directions from a linear center with rare curvature. Morphology DC consists of delicate blades that form well-developed  $60^{\circ}$ – $120^{\circ}$  semi-radial “bow-tie” to full  $360^{\circ}$  radial fans. Some fans comprise straight needles (3–10 mm), while others are feather-like to dendritic, with smaller curved branches emanating from the main needles.

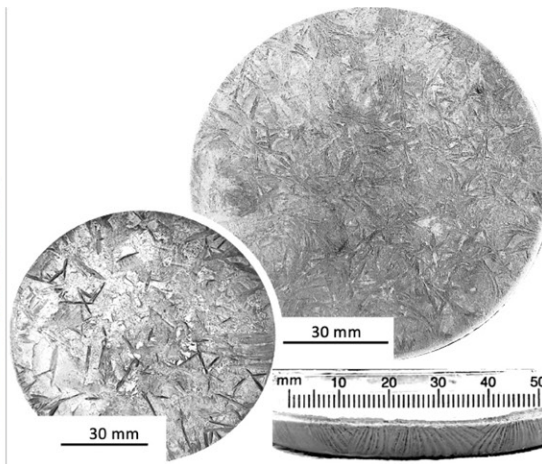
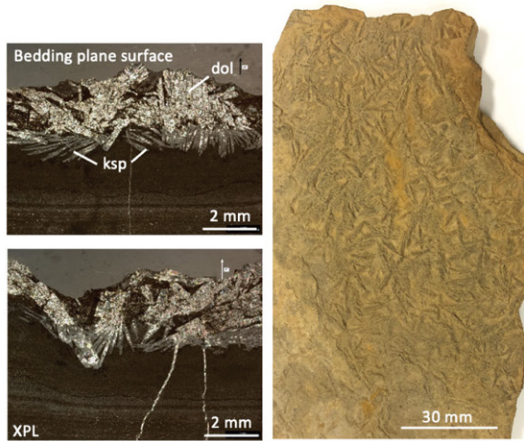
### Laboratory Simulation of Ice Growth in Sediment

Morphologies of experimental ice (formed at  $-15^{\circ}\text{C}$  in saturated to supersaturated mud) match the scale and form of bedding-plane impressions from the Usclas Formation (Fig. 2). The variable that most influences morphology is sediment water saturation, with a secondary influence from water chemistry. Morphology SR generally forms in mud saturated or supersaturated (for shorter, deeper impressions) with distilled water; FN forms in mud with very dilute NaCl (0.1%–0.5%)–saturated conditions, and DC forms in mud saturated with 0.5%–1% NaCl solution. Note that natural growth rates are much slower (0.01–0.1 in/hr [0.2–2.5 mm/hr];

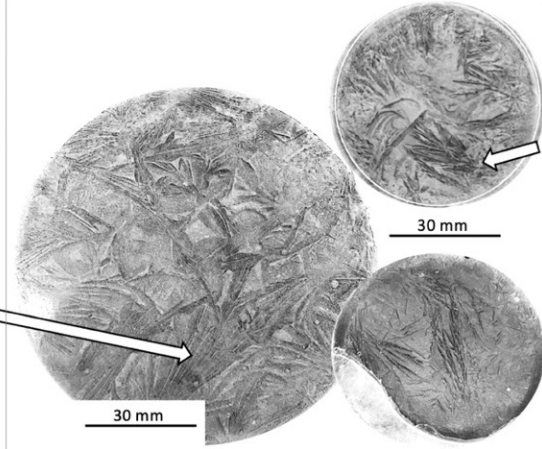
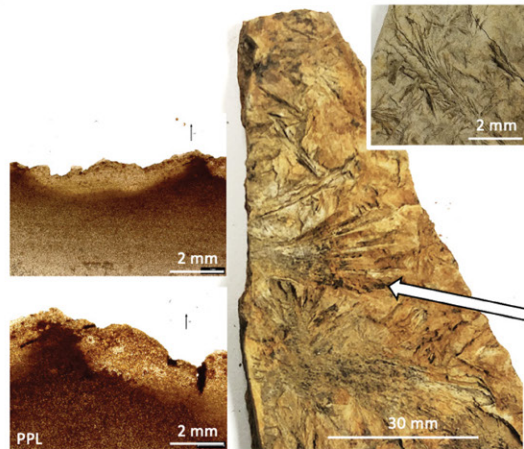
USCLAS FORMATION SAMPLES

EXPERIMENTAL RESULTS

MORPHOLOGY "SR"



MORPHOLOGY "FN"



MORPHOLOGY "DC"

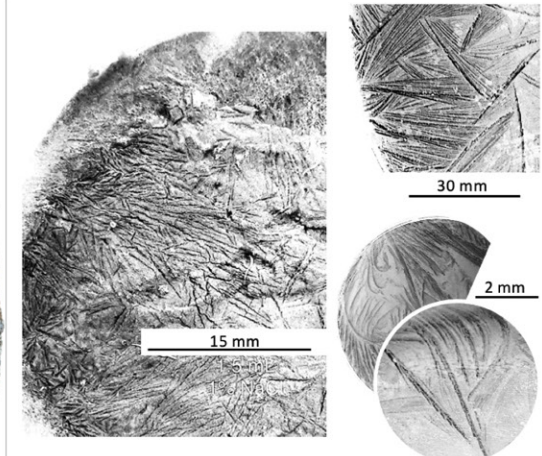
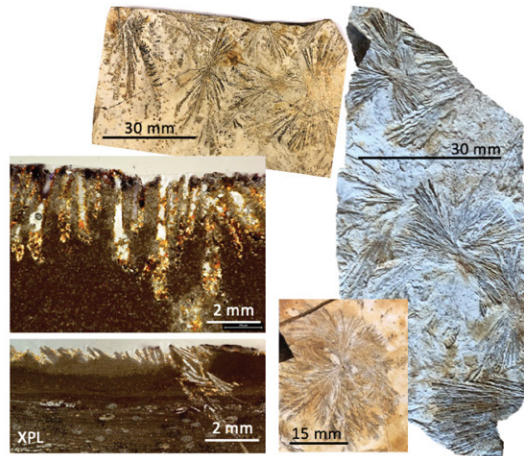


Figure 2. Summary of morphologic characteristics of features from the Usclas Formation (south-central France) (left) adjacent to examples from experimental results (right) that replicate features in each morphology, respectively (SR—stubby rods; FN—fanned needles; DC—delicate, complex). XPL—cross polarized light; PPL—plain polarized light; ksp—potassium feldspar; dol—dolomite.

Barns and Laudise, 1985), so the rate of freezing (relative to natural systems) is also a variable, but not within our experimental design.

**DISCUSSION**  
**Interpretation of Usclas Formation Features as Ice-Crystal Traces**

Empirical replication of the observed Usclas Formation morphologies using fully saturated mud beneath a film ( $\leq 1.5$  mm thick) of water (with as much as 1% NaCl) corroborates the interpretation that these features represent ice-crystal

molds. Furthermore, the common morphological features that define both ice-crystal traces from modern mudflats (e.g., Table 1; Figs. S2A–S2C) and inferred ice-crystal traces from the ancient record (e.g., Table 1; Figs. S2D–S2L) reinforce this interpretation. Generally, these characteristics include straight, tapered, needle-like traces in bundled to radial habits that exhibit intersecting or overlapping patterns. Experiments reproduced (in size and form) the defining characteristics of each morphology (Fig. 2), including the short, higher-relief features of morphology SR,  $60^{\circ}$ – $120^{\circ}$  fans

of FN, and delicate, radial blades and dendritic branches of DC. DC morphologies visually replicate irrefutable ice-crystal traces from modern playas (e.g., Fig. S2C). FN morphologies resemble shapes of both modern (e.g., Fig. S2B) and inferred Pleistocene ice-crystal traces (e.g., Figs. S2D and S2E) and cryostructures (e.g., Fig. S2F). The rod-like forms of SR resemble *Fucoides graphica* features referenced in early interpretations of peritidal ground ice (Hall, 1843; Clarke, 1918).

Empirical results show that the primary controls on crystal morphology (notably, aspect

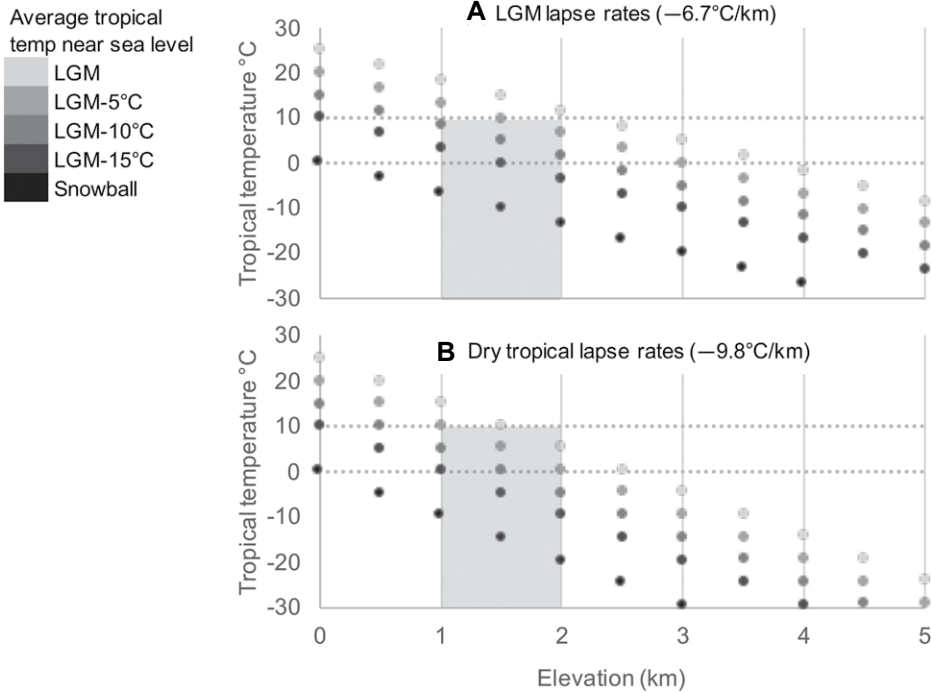


**Figure 3.** Plots of possible tropical temperature conditions in the Permian at different elevations using the same adiabatic lapse rate as the Last Glacial Maximum (LGM) ( $-6.7\text{ }^{\circ}\text{C}/\text{km}$ ; Loomis et al., 2017) (A) and “dry” tropical lapse rate ( $-9.8\text{ }^{\circ}\text{C}/\text{km}$ ; MacLennan et al., 2020) (B). Gray zone represents possible paleoelevations (within error) of the Lodève Basin at ca. 295 Ma during Usclas Formation deposition (see discussion in text). Average tropical temperatures near sea level range from LGM temperatures (lightest gray) to  $15\text{ }^{\circ}\text{C}$  cooler than LGM (darkest gray). LGM minus  $15\text{ }^{\circ}\text{C}$  is the coolest end of the range of estimates proposed by Soreghan et al. (2014) ( $0\text{--}15\text{ }^{\circ}\text{C}$  cooler than LGM) to have  $\sim 1000\text{ m}$  glacial conditions in western equatorial Pangea. Dotted horizontal lines represent average equatorial near-surface mean annual temperatures (MATs) ( $0\text{--}10\text{ }^{\circ}\text{C}$ ) that could support upland glaciation in low-latitude Pangea (Feulner, 2017).

ratio) are fluid saturation of the mud and water depth. Water chemistry also influences crystal shape, with more complex (curved, feathery, dendritic) forms (Fig. 2, morphology DC) resulting from dilute NaCl solutions ( $0.1\%\text{--}1\%$ ). Previous observations of ice crystallization in both laboratory (e.g., Allan, 1926; Mark, 1932; Reineck, 1955) and natural settings (e.g., Figs. S2A–S2C; Table 1; Reineck and Singh, 1980) also emphasized the influence of water saturation of the host sediment on crystal size and morphology. Deposition of the Usclas Formation coincides with rapid subsidence (Pfeifer et al., 2018) as well as fine (Appendix S2) sediment deposition (ash), enhancing preservation of the delicate traces (as in a *Lagerstätte*).

Odin (1986) interpreted the bedding-plane traces in the Usclas Formation as the result of evaporite (gypsum) crystallization, supported by other evidence for shallow water and dry conditions (e.g., desiccation features) elsewhere in this unit. The morphologies of the Usclas Formation traces, however, are inconsistent with the typical prismatic, pyramidal habits or “brain-like” textures of gypsum crystals (e.g., Magee, 1991) and cubic habits of common halite. Rare forms of gypsum, halite, barite, and other saline minerals (Appendix S4) can exhibit a fan-like or fibrous nature somewhat similar to individual Usclas Formation morphologies, but inconsistencies in scale

and form preclude an origin as evaporite minerals (Appendix S4). Additionally, all three morphologies (SR, FN, DC) co-occur in the Usclas Formation, which is also inconsistent with any one alternative interpretation. The ability to empirically reproduce all three (SR, FN, DC)—together with the striking resemblance to a variety of modern ice-crystal morphologies (Appendix S3)—leaves ice as the most parsimonious and conservative explanation for the formation of these features.

### Paleoclimate Implications for the Early Permian

Empirical replication of ice-crystal molds supports the inference that the ice crystals formed in—at most—very shallow films ( $<2\text{ mm}$ ) of water and displaced sediment downward and outward during growth. This is consistent with ephemeral freezing along paleo-shorelines of the Usclas Formation lake, and is common in modern playa lakes in climates subject to freezing temperatures (e.g., Fig. S2C) but unknown in low-elevation equatorial regions.

Ephemeral freezing during cold seasons and at equatorial latitudes during the early Permian implies either (1) substantial elevation to enable freezing temperatures, or (2) assuming low elevations, markedly cooler equatorial conditions than even those of the Last Glacial Maximum

(LGM). Perennial freezing conditions exist in the tropics today (with glaciers descending to  $\sim 4500\text{ m}$  elevation; Porter, 2001) and existed during the LGM (with glacial expansion to  $\sim 3500\text{ m}$  elevation, or very rarely, as low as  $2400\text{ m}$  in high-precipitation regions; Kaser and Osmaston, 2002; Hastenrath, 2009). In the southern Massif Central, paleoelevations at the time of Usclas Formation deposition (ca. 295–290 Ma) can be approximated ( $1\text{--}2\text{ km}$ ; Fig. 3) within the spatial and temporal bounds of existing data. The crustal thickness in the southern Massif Central ca. 308 Ma was  $\sim 45\text{ km}$  ( $\sim 30\text{ km}$  of present-day Variscan crust plus  $\sim 15\text{ km}$  overburden removed by ca. 285 Ma; Rabin et al., 2015; Pfeifer et al., 2018). Assuming a ratio of 1:6 for isostatic compensation of thickening, this corresponds to an elevation of  $\sim 2500\text{ m}$ , but subsequent extensional subsidence to gravity collapse ( $300\text{--}290\text{ Ma}$ ; Burg et al., 1994) would have further reduced the mean elevation of the Lodève Basin by  $\sim 500\text{--}1500\text{ m}$  (Sonder et al., 1987; Wolfe et al., 1998).

Moderate to low elevations ( $1\text{--}2\text{ km}$ ) for seasonal freezing in the Usclas Formation implies cooler tropical conditions than most models can replicate for low-latitude Pangea. The climatic forcing(s) necessary to impact tropical precipitation patterns and promote anomalously cold conditions in equatorial Pangea remain poorly understood (Heavens et al., 2015) but likely involved both short- and long-term factors. Average tropical air temperatures ( $25\text{ }^{\circ}\text{C}$ ) and lapse rates ( $-6.7\text{ }^{\circ}\text{C}/\text{km}$ ) from the LGM (e.g., Loomis et al., 2017) could not have produced even ephemeral freezing at  $<2\text{ km}$  elevations (Fig. 3). However, both (1) temperatures averaging  $\sim 5\text{ }^{\circ}\text{C}$  cooler than the LGM with an LGM lapse rate (Fig. 3A) and (2) LGM temperatures with a dry tropical lapse rate ( $-9.8\text{ }^{\circ}\text{C}/\text{km}$ ; MacLennan et al., 2020; Fig. 3B) are consistent with ephemeral freezing at elevations  $<2\text{ km}$ . The extreme continentality (and thus, seasonality) of the Lodève Basin depicted by its inland position in both Pangea B (Fig. 1; Kent and Muttoni, 2020) and Pangea A (e.g., Molli et al., 2020) would have produced a drier (steeper) lapse rate (Fig. 3B). On longer time scales, orbital variability and volcanism likely amplified paleoclimatic change during this time. For example, LPIA climate simulation of peak icehouse conditions shows that  $p\text{CO}_2 < 150\text{ ppm}$  under a cold summer orbit could have produced near-surface equatorial mean annual temperatures (MATs) of  $0\text{--}10\text{ }^{\circ}\text{C}$  (Feulner, 2017), consistent with upland glaciation and thus ephemeral freezing at lower elevations. Furthermore, Soreghan et al. (2019) hypothesized that frequent and widespread explosive volcanism in central and western Europe (at low latitude) at ca. 300 Ma may have intensified or sustained cool temperatures, even as  $p\text{CO}_2$  began to rise. Local evidence in support of coeval volcanism occurs in the Usclas Formation in the form of the altered, ash-like, illite-rich clay mineral compositions of mudstones containing the

inferred ice-crystal impressions and the tuffaceous units that directly overlie them (Fig. 1).

To date, examples of ice-crystal traces in the low-latitude geological record date exclusively from the upper Carboniferous–lower Permian (Table 1), calling for exploration of a potentially widespread phenomenon that has been long overlooked owing to the seeming implausibility of freezing conditions at relatively low elevations in equatorial latitudes of Pangea.

## CONCLUSIONS

Laboratory analyses empirically reproduce sediment impressions left by freezing of water-saturated mud and support the interpretation that morphologically identical features from the lower Permian Usclas Formation (Lodève Basin, France) represent ice-crystal traces. Evidence for films of ice on the paleoshoreline of a low-latitude lake records ephemeral freezing in equatorial Pangea during peak icehouse conditions (LPIA). Given the relatively low elevation (1–2 km) of the Lodève Basin during this time, these conditions require cold tropical temperatures (~5 °C cooler than those of the LGM) and/or lapse rates that exceeded those of the LGM. The forcing(s) necessary to promote cold climate conditions in equatorial Pangea remain enigmatic, but the extreme continentality of the Lodève Basin would have magnified strong seasonality. This work corroborates the presently sparse—yet temporally unique—recognition of low-latitude ice traces in the Phanerozoic (exclusively Permo-Carboniferous) record and calls for further investigation of evidence for anomalously cold equatorial temperatures and explanations thereof.

## ACKNOWLEDGMENTS

This research was supported by the U.S. National Science Foundation (NSF): NSF IRES grant 1658614 (G.S. Soreghan, M.J. Soreghan) and NSF grant 1338331 (G.S. Soreghan). Thanks to L. Alaniz, J. Mueller, J. Langston, S. Huntsman, E. Simpson, V. Smith, and K. Yeager for field assistance; and L. Hunt, A. Roche, and Z. Tomlinson for microprobe sample preparation and analysis. We thank M. Elwood-Madden, P. Getty, N. Heavens, J. Obrist-Farner, F. Oboh-Ikuenobe, M. Soreghan, J. Trop, C. Ver Straeten, and S. Voigt for discussions; and a special thanks to K. Benison, G. Dickens, and anonymous reviewers for their constructive feedback.

## REFERENCES CITED

Allan, J.A., 1926, Ice crystal markings: *American Journal of Science*, v. 11, p. 494–500, <https://doi.org/10.2475/ajs.s5-11.66.494>.

Barns, R.L., and Laudise, R.A., 1985, Size and perfection of crystals in lake ice: *Journal of Crystal Growth*, v. 71, p. 104–110, [https://doi.org/10.1016/0022-0248\(85\)90049-1](https://doi.org/10.1016/0022-0248(85)90049-1).

Becq-Giraudon, J.-F., Montenat, C., and Van Den Driessche, J., 1996, Hercynian high-altitude phenomena in the French Massif Central: Tectonic implications: *Palaeogeography, Palaeoclimatology, Palaeoecology*, v. 122, p. 227–241, [https://doi.org/10.1016/0031-0182\(95\)00081-X](https://doi.org/10.1016/0031-0182(95)00081-X).

Burg, J.-P., Van Den Driessche, J., and Brun, J.-P., 1994, Syn- to post-thickening extension in the Variscan Belt of Western Europe: Modes and structural

consequences: *Comptes Rendus de l'Academie des Sciences Paris*, v. 319, p. 1019–1032.

Clarke, J.M., 1918, Strand and undertow markings of Upper Devonian time as Indications of the prevailing climate, in *Thirteenth Report of the Director of the State Museum and Science Department: New York State Museum Bulletin* 196, p. 199–210.

Domeier, M., and Torsvik, T.H., 2014, Plate tectonics in the late Paleozoic: *Geoscience Frontiers*, v. 5, p. 303–350, <https://doi.org/10.1016/j.gsf.2014.01.002>.

Evans, M.E., Pavlov, V., Veselovsky, R., and Fetisova, A., 2014, Late Permian paleomagnetic results from the Lodève, Le Luc, and Bas-Argens Basins (southern France): *Magnetostratigraphy and geomagnetic field morphology: Physics of the Earth and Planetary Interiors*, v. 237, p. 18–24, <https://doi.org/10.1016/j.pepi.2014.09.002>.

Feulner, G., 2017, Formation of most of our coal brought Earth close to global glaciation: *Proceedings of the National Academy of Sciences of the United States of America*, v. 114, p. 11,333–11,337, <https://doi.org/10.1073/pnas.1712062114>.

Hall, J., 1843, *Geology of New-York: Part IV, Comprising the Survey of the Fourth Geological District: Albany, New York, Carroll and Cook*, 683 p.

Hastenrath, S., 2009, Past glaciation in the tropics: *Quaternary Science Reviews*, v. 28, p. 790–798, <https://doi.org/10.1016/j.quascirev.2008.12.004>.

Heavens, N.G., Mahowald, N.M., Soreghan, G.S., Soreghan, M.J., and Shields, C.A., 2015, A model-based evaluation of tropical climate in Pangea during the late Palaeozoic icehouse: *Palaeogeography, Palaeoclimatology, Palaeoecology*, v. 425, p. 109–127, <https://doi.org/10.1016/j.palaeo.2015.02.024>.

Julien, A., 1895, Ancien glaciers de la période houillère dans le plateau central de la France: *Annuaire du Club Alpin Français*, v. 21, p. 1–28.

Kaser, G., and Osmaston, H., 2002, *Tropical Glaciers: Cambridge, UK, Cambridge University Press*, 207 p.

Kent, D.V., and Muttoni, G., 2020, Pangea B and the Late Paleozoic Ice Age: *Palaeogeography, Palaeoclimatology, Palaeoecology*, v. 553, 109753, <https://doi.org/10.1016/j.palaeo.2020.109753>.

Loomis, S.E., Russell, J.M., Verschuren, D., Morrill, C., De Cort, G., Sinnighe Damsté, J.S., Olago, D., Eggermont, H., Street-Perrott, F.A., and Kelly, M.A., 2017, The tropical lapse rate steepened during the Last Glacial Maximum: *Science Advances*, v. 3, e1600815, <https://doi.org/10.1126/sciadv.1600815>.

MacLennan, S.A., Eddy, M.P., Merschat, A.J., Mehra, A.K., Crockford, P.W., Maloof, A.C., Southworth, C.S., and Schoene, B., 2020, Geologic evidence for an icehouse Earth before the Sturtian global glaciation: *Science Advances*, v. 6, eaay6647, <https://doi.org/10.1126/sciadv.aay6647>.

Magee, J.W., 1991, Late Quaternary lacustrine, groundwater, aeolian and pedogenic gypsum in the Prungle Lakes, southeastern Australia: *Palaeogeography, Palaeoclimatology, Palaeoecology*, v. 84, p. 3–42, [https://doi.org/10.1016/0031-0182\(91\)90033-N](https://doi.org/10.1016/0031-0182(91)90033-N).

Mark, W.D., 1932, Fossil impressions of ice crystals in Lake Bonneville beds: *The Journal of Geology*, v. 40, p. 171–176, <https://doi.org/10.1086/623932>.

Molli, G., Brogi, A., Caggianelli, A., Capezzuoli, E., Liotta, D., Spina, A., and Zibra, I., 2020, Late Palaeozoic tectonics in Central Mediterranean: A reappraisal: *Swiss Journal of Geosciences*, v. 113, 23, <https://doi.org/10.1186/s00015-020-00375-1>.

Montenat, C., and Dolle, P., 1986, Des traces de gel dans l'Autunien du Midi de la France?, in *Paleozoïque Supérieur Continental Conference: Lille*, p. 51 (abstract).

Odin, B., 1986, Les formations permienne, Autunien supérieur à Thuringienne, du "Bassin" de Lodève (Hérault, France): *Stratigraphie, minéralogie, paléoenvironnements, corrélations* [Ph.D. thesis]: Aix-Marseille, France, Université Aix-Marseille III, 392 p.

Pfeifer, L.S., Soreghan, G.S., Pochat, S., Van Den Driessche, J., and Thomson, S.N., 2018, Permian exhumation of the Montagne Noire core complex recorded in the Graissessac-Lodève Basin, France: *Basin Research*, v. 30, p. 1–14, <https://doi.org/10.1111/bre.12197>.

Pfeifer, L.S., Soreghan, G.S., Pochat, S., and Van Den Driessche, J., 2020, Loess in eastern equatorial Pangea archives a dusty atmosphere and possible upland glaciation: *Geological Society of America Bulletin*, v. 133, p. 379–392, <https://doi.org/10.1130/B35590.1>.

Pochat, S., and Van Den Driessche, J., 2011, Filling sequence in Late Paleozoic continental basins: A chimera of climate change? A new light shed given by the Graissessac-Lodève basin (SE France): *Palaeogeography, Palaeoclimatology, Palaeoecology*, v. 302, p. 170–186, <https://doi.org/10.1016/j.palaeo.2011.01.006>.

Porter, S.C., 2001, Snowline depression in the tropics during the Last Glaciation: *Quaternary Science Reviews*, v. 20, p. 1067–1091, [https://doi.org/10.1016/S0277-3791\(00\)00178-5](https://doi.org/10.1016/S0277-3791(00)00178-5).

Rabin, M., Trap, P., Carry, N., Fréville, K., Cenk-Tok, B., Lobjoie, C., Goncalves, P., and Marquer, D., 2015, Strain partitioning along the anatectic front in the Variscan Montagne Noire massif (southern French Massif Central): *Tectonics*, v. 34, p. 1709–1735, <https://doi.org/10.1002/2014TC003790>.

Reineck, H.E., 1955, *Marken, Spuren und Fährten in den Waderner Schichten (ro) bei Martinstein/Nahe: Neues Jahrbuch für Geologie und Paläontologie, Abhandlungen*, v. 101, p. 75–90.

Reineck, H.E., and Singh, I.B., 1980, *Depositional Sedimentary Environments: Berlin, Springer-Verlag*, 551 p., <https://doi.org/10.1007/978-3-642-81498-3>.

Sonder, L.J., England, P.C., Wernicke, B.P., and Christiansen, R.L., 1987, A physical model for Cenozoic extension of western North America, in Coward, M.P., et al., eds., *Continental Extensional Tectonics: Geological Society [London] Special Publication* 28, p. 187–201, <https://doi.org/10.1144/GSL.SP.1987.028.01.14>.

Soreghan, G.S., Soreghan, M.J., Poulsen, C.J., Young, R.A., Eble, C.F., Sweet, D.E., and Davogusto, O.C., 2008, Anomalous cold in the Pangean tropics: *Geology*, v. 36, p. 659–662, <https://doi.org/10.1130/G24822A.1>.

Soreghan, G.S., Sweet, D.E., and Heavens, N.G., 2014, Upland glaciation in tropical Pangea: Geologic evidence and implications for late Paleozoic climate modeling: *The Journal of Geology*, v. 122, p. 137–163, <https://doi.org/10.1086/675255>.

Soreghan, G.S., Soreghan, M.J., and Heavens, N.G., 2019, Explosive volcanism as a key driver of the late Paleozoic ice age: *Geology*, v. 47, p. 600–604, <https://doi.org/10.1130/G46349.1>.

Torsvik, T.H., et al., 2012, Phanerozoic polar wander, palaeogeography and dynamics: *Earth-Science Reviews*, v. 114, p. 325–368, <https://doi.org/10.1016/j.earscirev.2012.06.007>.

Wolfe, J.A., Forest, C.E., and Molnar, P., 1998, Paleobotanical evidence of Eocene and Oligocene paleoaltitudes in midlatitude western North America: *Geological Society of America Bulletin*, v. 110, p. 664–678, [https://doi.org/10.1130/0016-7606\(1998\)110<0664:PEOEAO>2.3.CO;2](https://doi.org/10.1130/0016-7606(1998)110<0664:PEOEAO>2.3.CO;2).

Printed in USA